21 Biophysical Phenomics Reveals Functional Building Blocks of Plants Systems Biology: a Case Study for the Evaluation of the Impact of Mycorrhization with *Piriformospora indica* *

R.J. Strasser, M. Tsimilli-Michael, D. Dangre, and M. Rai

21.1 Introduction

Soil microbial activity is a main parameter in ecosystem functions. Arbuscular mycorrhiza fungi are mutualistic microsymbionts of about 90% of higher plants in natural, semi-natural and agricultural plant communities. As mycorrhizosphere systems can be tailored to help plants to survive in nutrient-deficient, degraded habitats or during stress periods, they are highly advantageous in sustainable agriculture. However, the success of this practise, as for any microbial inoculation, depends strongly on the effectiveness of mycorrhization, which depends on complex interactions between plant and symbiont.

Mycorrhization has multiple effects on the physiology of the plant at different levels. We focus our interest on the responses of the photosynthetic apparatus and especially on photosystem (PS) II (see e.g. Tsimilli-Michael et al. 2000) which is well known to be a component of the plant system highly sensitive to any stress.

Our approach for the evaluation of the effectiveness of mycorrhization, which we term *biophysical phenomics*, is based on the description of an in vivo vitality analysis (behaviour/performance) of PSII, i.e. the description of a biophysical phenotype. The tools that provide access to this phenotyping, termed the "JIP-test", are based on the analysis of the fast fluorescence kinetics O-J-I-P exhibited

Reto J. Strasser, Merope Tsimilli-Michael: Laboratory of Bioenergetics, University of Geneva, Chemin des Embrouchis 10, CH-1254 Jussy-Geneva, Switzerland,
email: Reto.Strasser@bioveg.unige.ch

Merope Tsimilli-Michael: Ath. Phylactou 3, CY-1100, Nicosia, Cyprus,
email: tsimicha@spidernet.com.cy

Devanand Dangre, Mahendra Rai: Department of Biotechnology, SGB Amravati University, Amravati-444602, Maharashtra, India,
email: mkrai123@rediffmail.com; pmkrai@hotmail.com

* Dedicated to the memory of Hannes Schuepp, a great scientist and a wonderful person.

Soil Biology, Volume 11
Advanced Techniques in Soil Microbiology
A. Varma, R. Oelmüller (Eds.)
© Springer-Verlag Berlin Heidelberg 2007

by all oxygenic photosynthetic organisms upon illumination (for reviews, see Strasser et al. 2000, 2004).

Moreover, in our analysis, we show that biophysical phenotyping, which refers to the system macrostate, allows us to recognise and evaluate impacts on the function and (re)distribution of the heterogeneous microstates – functional building blocks – whose balance defines the macrostate (Strasser and Tsimilli-Michael 2005).

We also present, as an application of our approach, a case study of the beneficial role of the emerging growth booster and in vitro-cultivable *Piriformospora indica* (Varma et al. 1999) on chick peas (*Cicer arietinum* L. Chafa variety) exposed to cadmium stress, which we further compare with the impact of typical arbuscular mycorrhiza fungi (*Glomus mosseae*, *Glomus caledonium*).

21.2 Biophysical Phenomics of the Fast Fluorescence Rise O-J-I-P

21.2.1 The Energy Cascade in the Photosynthetic Apparatus

A simplified scheme for the energy cascade in photosystem II of the photosynthetic apparatus is presented in Fig. 21.1 (modified after Epitalawage et al. 2003). Not only solar energy but any light energy of suitable wavelengths, i.e. wavelengths that can be absorbed by chlorophyll and accessory pigments, has the same fate. In the energy conservation pathway, the flux of photons is transformed sequentially to a flux of excitons, a flux of electrons and a flux of molecules. The electron flow is coupled to the formation of adenosine triphosphate (ATP), which is a high-energy compound. The end-products are molecular oxygen (O_2), evolved by water (H_2O) splitting, and sugars, formed from carbon dioxide (CO_2). Part of the excitation is not conserved; it is dissipated, mainly as heat and less as fluorescence emission by chlorophyll (Chl) *a*. As the kinetics of Chl *a* fluorescence reflect changes in the function and structure of PSII and, concomitantly, changes in the whole electron transport chain, they provide a very useful, non-invasive tool for the investigation of the behaviour and performance of the photosynthetic apparatus.

21.2.2 Microstates – Functional Building Blocks of Photosynthesis

According to open system thermodynamics, the Gibb's energy, linked to biochemical activity (quantity term), and the entropy-related energy component,

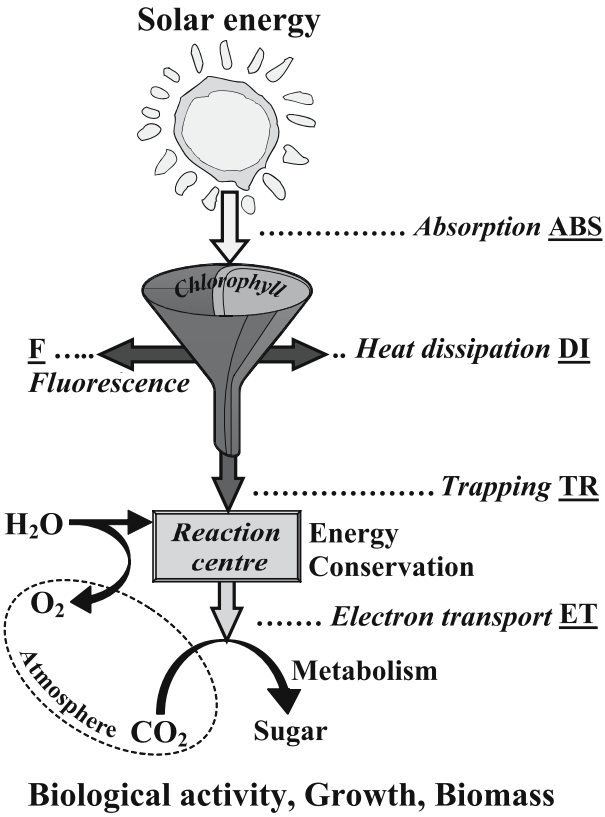

Fig. 21.1 A simplified scheme for the energy cascade in photosystem II (PSII) of the photosynthetic apparatus (modified after Epitalawage et al. 2003). Light absorption (ABS) creates excited chlorophyll. Part of the excitation energy is dissipated, mainly as heat (heat dissipation, *DI*) and less as fluorescence emission (F); another part is channelled to the reaction centre (trapping, TR) to be converted to redox energy (*Energy Conservation*), with the simultaneous evolution of oxygen (O2) by water (H2O) splitting. The redox energy creates electron transport (ET), which, via PSI (not shown), leads ultimately to CO_2 fixation into sugars (*Metabolism*)

linked to the structure, complexity and organization of the system (quality term) follow optimization strategies, potentially establishing steady-states (stability term) under given conditions (see Strasser and Tsimilli-Michael 2005).

Recognizing the high complexity and heterogeneity of the photosynthetic system in nature (see also Strasser 1985; Strasser and Tsimilli-Michael 1998), we propose that its apparent state is a heterogeneous macrostate, determined by the statistical distribution of microstates, as listed in the model shown in Fig. 21.2 (modified after Strasser and Tsimilli-Michael 2005): architecture of PSII and PSI antenna, i.e. size and connectivity among units (grouped/separate), light-harvesting complexes (LHC II and I), kinase-catalyzed migration from PSII to PSI of an LHC component when phosphorylated (LHC~P), spill-over from PSII to PSI antenna, types of electron donation to PSII raction centers (from wa-

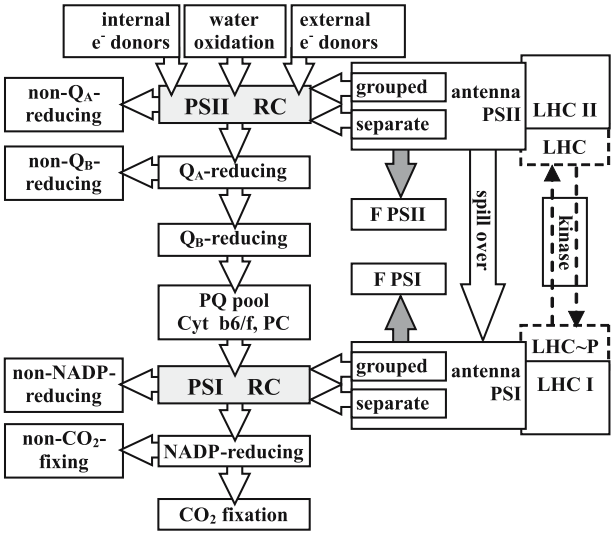

Fig. 21.2 Heterogeneity of microstates/functional units, whose balance determines the macrostate of the photosynthetic system (modified after Strasser and Tsimilli-Michael 2005). For details, see text

ter oxidation or internal/external donors), Q_A^- reducing reaction centers (RC) or non-Q_A^- reducing (heat sinks), Q_B^- reducing or non-Q_B^- reducing (slow Q_A^- re-oxidizing) units, states of intermediate electron carriers (PQ pool, Cytb6/f, PC), splitting of PSI acceptor side, in non-NADP-reducing pathways and NADP-reducing pathways, the latter further split in non-CO_2-fixing and towards CO_2 fixation. For any steady-macrostate (optimal/adapted), the balance of mechanisms governing the distribution of microstates is equivalent to optimizations of quantity, quality and stability, which are interrelated, governed by the genetics of the system, its resources and its environment. Concomitantly, stress is any disturbance of the achieved balance, upon which the system undergoes microstate changes towards a new optimal balance, i.e. a new macrostate (Strasser and Tsimilli-Michael 2005).

21.2.3 Measuring Fluorescence Transients with PEA, Handy-PEA and FIM- Fluorimeters

Chl *a* fluorescence transients exhibited by any photosynthetic material are measured by a PEA (Plant Efficiency Analyser) or Handy-PEA fluorimeter (Hansatech Instruments, King's Lynn, UK; Fig. 21.3) or FIM fluorimeter (Fluorescence Induction Meter 1500; ADC, Hoddesdon, UK). The transients are induced by a red light (peak at 650 nm) of 600 W m^{-2} (equivalent to 3200 μE s^{-1} m^{-2}) provided by an array of six (PEA and FIM fluorimeters) or three (Handy-PEA fluorimeter) light-emitting diodes, and recorded for 1 s with 12 bit resolution. The data

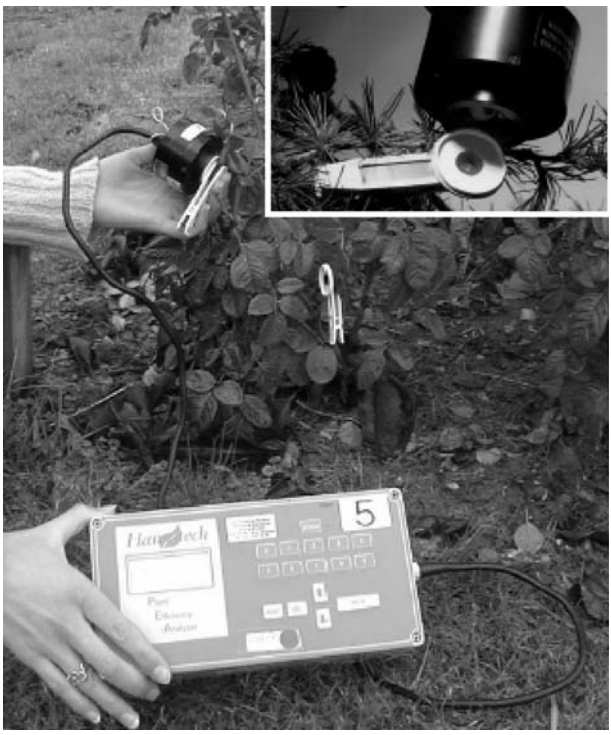

Fig. 21.3 The PEA (Handy-PEA) fluorimeter used for our studies. The photo is from in situ measurements, with the clips already put on the leaves to dark-adapt them. The insert shows the sensor of the instrument, which provides, by LEDs, the red actinic light (650 nm) and collects the fluorescence signals

acquisition in the PEA and FIM fluorimeters is every 10 μs for the first 2 ms, every 1 ms between 2 ms and 1000 ms and every 100 ms thereafter (for further details, see Strasser et al. 1995; for reviews, see Strasser et al. 2000, 2004), while in the Handy-PEA fluorimeter it is every 10 μs (in the interval 10 μs to 0.3 ms), every 0.1 ms (0.3–3.0 ms), every 1 ms (3–30 ms), every 10 ms (30–300 ms), etc. (see e.g. Tóth et al. 2005). The first reliable measurement with PEA and FIM fluorimeters is at 50 μs, while with the Handy-PEA fluorimeter it is at 20 μs.

21.2.4 How Fluorescence Kinetics Provide an Insight to the Microstates – Functional Blocks of PSII

21.2.4.1 Qualitative Screening of Many Samples

Screening of many samples in situ by recording Chl *a* fluorescence transients is a very simple task. Figure 21.4 depicts Chl *a* fluorescence transients of dark-adapted leaves of *Hedera* (left panel) and *Shefflera* (right panel), measured with

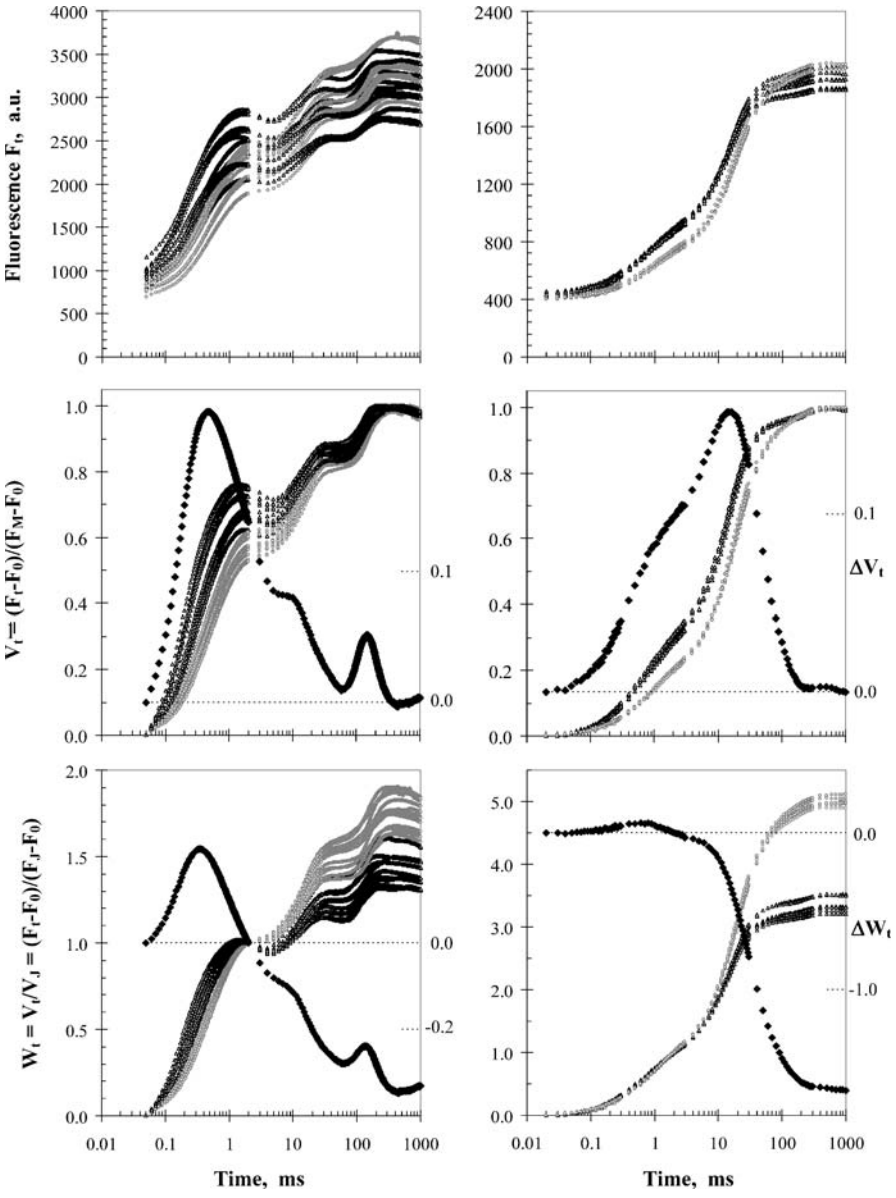

Fig. 21.4 Chl *a* fluorescence transients of dark adapted leaves of *Hedera* (*left panels*) and *Shefflera* (*right panels*), measured with PEA and Handy-PEA fluorimeters respectively. Young leaves (*black open triangles*) and mature leaves (*open grey circles*) from both plants were measured. The transients, induced by saturating red actinic light (peak at 650 nm) of 600 W m^{-2} (equivalent to about 3000 μE s^{-1} m^{-2}), are plotted on a logarithmic time-scale. The plots in the *upper panels* depict the kinetics of the raw fluorescence data, F_t. The kinetics of the relative variable fluorescence V_t and W_t, calculated from the raw data as $V_t = (F_t–F_0)/(F_M–F_0)$ and $W_t = V_t/V_J = (F_t–F_0)/(F_J–F_0)$, are depicted in the plots of the *middle and lower panels* respectively (*left axis*). In the plots of V_t and W_t, the corresponding differences ΔV_t and ΔW_t, between the average transients of young and mature leaves (young minus mature) are also plotted (black closed diamonds; *right axis*). For other details, see text

PEA and Handy-PEA fluorimeters, respectively. Young leaves (black open triangles) and mature leaves (open grey circles) from both plants were measured. The transients, induced by saturating red actinic light (peak at 650 nm) of 600 W m^{-2} (equivalent to about 3000 μE s^{-1} m^{-2}), are plotted on a logarithmic time-scale.

The plots in the upper panels depict the kinetics of the raw fluorescence data, F_t. The first to observe is that all the transients are polyphasic with, however, differences between the two species. We can also clearly observe that *Shefflera* (right panel) exhibits a high homogeneity among samples, which permits the distinction between young and mature leaves, while in *Hedera* possible differences are hidden under the wide heterogeneity between samples.

However, when we transform the kinetics of the raw data to the kinetics of the relative variable fluorescence $V_t = (F_t–F_0)/(F_M–F_0)$ or $W_t = V_t/V_J = (F_t–F_0)/(F_J–F_0)$ [for the definition of terms and symbols, see text below as well as Fig. 21.5 and Table 21.1], we can see in the respective plots of the middle and lower panels a clear distinction between young and mature leaves for both species. In these plots, the corresponding differences ΔV_t and ΔW_t, between the average transients of young and mature leaves (young minus mature) are also plotted (black closed diamonds; secondary vertical axis).

21.2.4.2
The Typical O-J-I-P Fluorescence Transient: Definition of Steps and Selection of Fluorescence Data for the JIP-Test

The Chl *a* fluorescence transient, known as the Kautsky transient (Kautsky and Hirsh 1931), consists of a rise completed in less than one second and a subsequent slower decline towards a steady state. Our method presented here utilises only the fast rise that is generally accepted to reflect the accumulation of the reduced form of the primary quinone acceptor Q_A, otherwise the closure of the reaction centres (RCs), which is the net result of Q_A reduction due to PSII activity and Q_A^- reoxidation due to photosystem I (PSI) activity. When the photosynthetic sample is kept for a few minutes in the dark, Q_A is fully oxidised, hence the RCs are all open, and the fluorescence yield at the onset of illumination is denoted as F_0 (minimal fluorescence). The maximum yield F_P at the end of the fast rise, depending on the achieved reduction–oxidation balance, acquires its maximum possible value – denoted as F_M – if the illumination is strong enough to ensure the closure of all RCs. A lot of information has been driven during the past 70 years from the fluorescence transient (for reviews, see Papageorgiou 1975; Briantais et al. 1986; Govindjee et al. 1986; Krause and Weiss 1991; Dau 1994; Govindjee 1995; Strasser et al. 2000, 2004).

Transients recorded with high time-resolution fluorimeters, e.g. the PEA- or Handy-PEA instrument that we use, have provided additional and/or more accurate information (Strasser and Govindjee 1992; Strasser et al. 1995; for reviews, see Strasser et al. 2000, 2004). The fluorescence rise kinetics was shown to be polyphasic, clearly exhibiting, when plotted on a logarithmic time-scale,

Table 21.1 Summary of terms, definitions and formulae used by the JIP-test

Experimental signals	Symbol	Formula
Minimal fluorescence intensity[a]	F_0	
Maximal fluorescence intensity	F_M	
Fluorescence intensity at 2 ms (J-step)	F_J	
Fluorescence intensity at 30 ms (I-step)	F_I	
Fluorescence intensity at 300 μs	$F_{300\mu s}$	
Normalised signals		
Maximum variable fluorescence	F_V	$= F_M - F_0$
Relative variable fluorescence (from F_0 to F_M)	V_t	$= (F_t - F_0) / (F_M - F_0)$
Relative variable fluorescence (from F_0 to F_J)	W_t	$= (F_t - F_0) / (F_J - F_0)$
Relative variable fluorescence at the J-step	V_J	$= (F_J - F_0) / (F_M - F_0)$
Relative variable fluorescence at the I-step	V_I	$= (F_I - F_0) / (F_M - F_0)$
Initial slope[a] of the $V = f(t)$ transient: $M_0 = (\Delta V/\Delta t)_0 \cong (dV/dt)_0 = [dQ_A^-/Q_{A,total})/dt]_0 =$ initial rate of primary photochemistry	M_0	$= 4\times (F_{300\mu s} - F_0) / (F_M - F_0)$
Specific fluxes: energy fluxes per reaction centre		
Specific flux for absorption	ABS/RC	$= (M_0/V_J) / [1 - (F_0/F_M)]$
Specific flux for trapping[a]	TR_0/RC	$= (M_0/V_J)$
Specific flux for dissipation[a]	DI_0/RC	$=$ (ABS/RC) $-$ (TR_0/RC)
Specific flux for electron transport[a]	ET_0/RC	$= (M_0/V_J) \times (1 - V_J)$
Yields or ratios of fluxes		
Maximum quantum yield[a] of primary photochemistry: $\varphi_{Po} \equiv TR_0/ABS$	φ_{Po}	$= [1 - (F_0/F_M)]$
Maximum yield[a] of electron transport: $\varphi_{Eo} \equiv ET_0/ABS$	φ_{Eo}	$= [1 - (F_0/F_M)] \times (1 - V_J)$
Efficiency[a] of a trapped exciton to move an electron into the electron transport chain further than Q_A^- : $\psi_0 \equiv ET_0/TR_0$	ψ_0	$= (1 - V_J)$

[a] At the onset of illumination (at 50 μs for PEA and FIM, or at 20 μs for Handy-PEA, in which case the initial slope must be calculated between 20 μs and 270 μs)

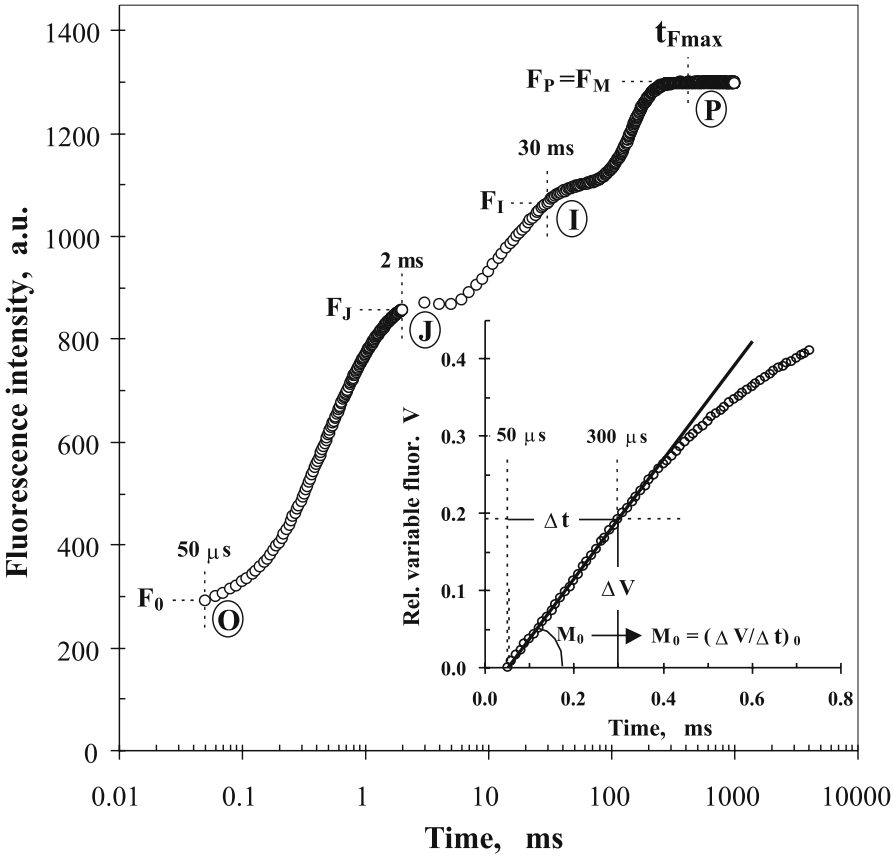

Fig. 21.5 A typical Chl *a* polyphasic fluorescence rise O-J-I-P, exhibited by higher plants. The transient is plotted on a logarithmic time-scale from 50 µs to 1 s. The marks refer to the selected fluorescence data used by the JIP-test for the calculation of structural and functional parameters. The signals are: the fluorescence intensity F_0 (at 50 µs), the fluorescence intensities F_J (at 2 ms) and F_I (at 30 ms) and the maximal fluorescence intensity $F_P = F_M$ (at t_{Fmax}). The insert presents the transient expressed as the relative variable fluorescence $V = (F–F_0)/(F_M–F_0)$ vs time, from 50 µs to 0.75 ms on a linear time-scale, demonstrating how the initial slope, also used by the JIP-test, is calculated: $M_0 = (dV/dt)_0 \cong (\Delta V/\Delta t)_0 = (V_{300\mu s})/(0.25\ ms)$

the steps J (at 2 ms) and I (at 30 ms) between the initial O (F_0) and maximum P level (F_P). Moreover, a much more precise detection of F_0 is achieved, as well as the detection of the initial slope, which offers a link to the maximum rate of photochemical reaction.

Despite differences among species (as e.g. shown in Fig. 21.4), all oxygenic photosynthetic material investigated so far using this method show this polyphasic rise, labelled O-J-I-P. A typical Chl *a* fluorescence transient O-J-I-P is shown in Fig. 21.5, plotted on a logarithmic time-scale. The following original data are utilised by the JIP-test: the maximal measured fluorescence intensity,

F_P, equal here to F_M since the excitation intensity is high enough to ensure the closure of all RCs of PSII; the fluorescence intensity at 50 μs considered as the intensity F_0 when all RCs are open; the fluorescence intensity at 300 μs ($F_{300\mu s}$) required for the calculation of the initial slope $M_0 = (dV/dt)_0 \cong (\Delta V/\Delta t)_0$ of the relative variable fluorescence (V) kinetics (see insert in Fig. 21.5); the fluorescence intensities at 2 ms (J-step) denoted as F_J, and at 30 ms (I-step) denoted as F_I (for reviews, see Strasser et al. 2000, 2004).

21.2.4.3
The O-L-K-J-I-H-G-P Fluorescence Transient: From Steps to Bands

As shown in Fig. 21.4, the kinetics of ΔV_t and ΔW_t (where V_t and W_t are different expressions of relative variable fluorescence) reveal bands hidden in the J- and I-steps of the fluorescence kinetics F_t, which are much richer in information than the original O-J-I-P.

Figure 21.6, which utilises the results of a stress study – nitrogen deficiency in cowpea plants (*Vigna unguiculata* L) – reported by Schmitz et al. (2001), offers a detailed presentation of these bands, regarding their position and labelling and their relation with the main steps. (Note: the transients are here presented as kinetics of ΔV_t; choosing ΔW_t would lead to the resolution of the same bands, as can be seen in Fig. 21.4). The sequence of events is distinguished in single-turnover and multiple-turnover events. Moreover, the main information that can be derived from each band is depicted, namely information concerning: Q_A, the oxidised primary quinone acceptor; p_{2G}, the overall grouping probability within PSII antenna; OEC, the oxygen-evolving complex; Q_B^-, the reduced (one electron) secondary quinone acceptor; Q_B^{2-}, the reduced (two electrons) secondary quinone acceptor; Q_BH_2, the protonated secondary quinone acceptor; EC_{red}, the fully reduced electron carriers.

One can easily see that this list of derivable information provides an insight to microstates – functional building blocks of photosynthesis, to which we deconvolute (see Fig. 21.2) the macrostate – biophysical phenotype.

21.2.4.4
The JIP-Test: Conversion of Experimental Signals to Biophysical Parameters and the Performance Index

For the evaluation of the impact of any stress and, similarly, of mycorrhizosphere activity on plants, we apply the "JIP-test", which provides a quantitative analysis of the in vivo vitality – behaviour/performance – of PSII, i.e. a quantitative description of the biophysical phenotype – macrostate, by accessing the different microstates – functional building blocks. The "JIP-test" is an analysis of the fast fluorescence kinetics O-J-I-P exhibited by all oxygenic photosynthetic

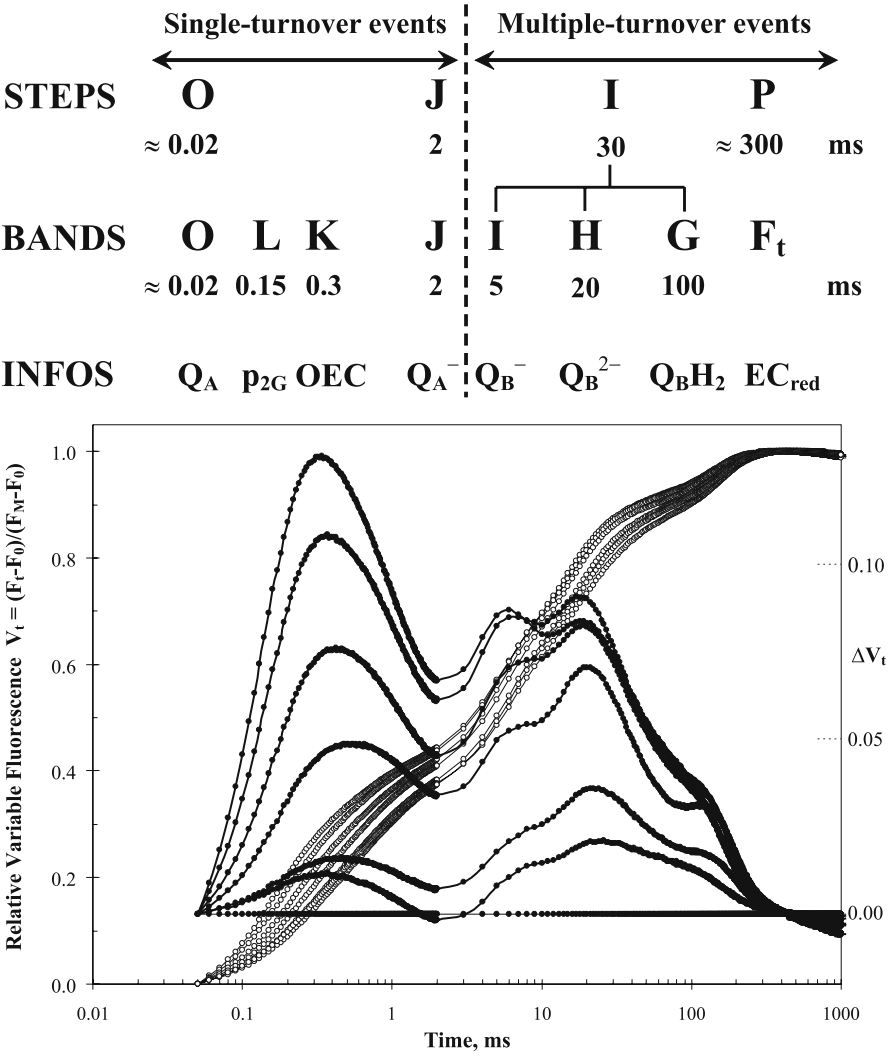

Fig. 21.6 Chlorophyll *a* fluorescence transients exhibited by dark-adapted leaves of cowpea plants (*Vigna unguiculata* L) grown at different KNO_3 concentrations (based on data from Schmitz et al. 2001) are presented as kinetics of relative variable fluorescence $V_t = (F_t–F_0)/(F_M–F_0)$, *open circles*, *left axis*, and as difference kinetics, ΔV_t, i.e. nitrogen deficient minus control (*closed circles*, *right axis*; see also legend of Fig. 21.4), where the extent of deficiency increases form bottom to top. The transients show the typical basic *STEPS* O-J-I-P (see also Fig. 21.5) while, as demonstrated in the *upper panel*, the difference transients reveal the full sequence of *BANDS* O-L-K-J-I-H-G-P (P or any F_t), which is much richer in information (for the L-band, see Fig. 21.8). *INFOS* refer to the main information that can be derived by each band, i.e. information concerning Q_A (oxidised primary quinone acceptor), p_{2G} (overall grouping probability within PSII antenna), OEC (oxygen evolving complex), Q_B^- -(reduced secondary quinone acceptor, one electron), Q_B^{2-} (reduced secondary quinone acceptor, two electrons), Q_BH_2 (protonated secondary quinone acceptor) and EC_{red} (fully reduced electron carriers). The *vertical dashed line* separates the phase of single-turnover events of primary photochemistry from that of multiple turnover events

organisms upon illumination, based on a simple model and the Theory of Energy Fluxes in Biomembranes (Strasser 1978, 1981). It is well documented that the shape of the O-J-I-P transient and its analysis by the JIP-test are efficient biophysical tools, not only in the recognition and evaluation of the beneficial role of mycorrhiza symbiosis on PSII activity (which we also approach as stress – see Tsimilli-Michael and Strasser 2002; see also Tsimilli-Michael et al. 2000) but, much more generally, in the biophysical phenotyping of the photosynthetic apparatus of a plant under any stress, biotic (e.g. Tsimilli-Michael et al. 2000) or abiotic, i.e. any stress caused by changes in different environmental conditions, e.g. light intensity, temperature, drought, atmospheric CO_2 or ozone elevation, chemical influences (Srivastava and Strasser 1995, 1996; Srivastava et al. 1997; Tsimilli-Michael et al. 1995, 1996, 1999, 2000; Tsimilli-Michael and Strasser 2001; Van Rensburg et al. 1996; Krüger et al. 1997; Ouzounidou et al. 1997; Clark et al. 1998, 2000; Van Heerden et al. 2003), even by diurnal changes (Strasser and Tsimilli-Michael 2001), as well as by senescence (Prakash et al. 2003). For a review, see Strasser et al. (2004).

The "JIP-test", which is a conversion of fluorescence data (selected as described above in 21.2.4.2; see also Fig. 21.5) to biophysical parameters and the performance index, is schematically presented in Fig. 21.7 and analytically in Table 21.1.

The biophysical parameters, all referring to time zero (onset of fluorescence induction) are: (a) the specific energy fluxes (per reaction centre, RC) for absorption (ABS/RC), trapping (TR_0/RC), dissipation (DI_0/RC = ABS/RC – TR_0/RC; not shown in Fig. 21.7, but see Table 21.1) and electron transport (ET_0/RC), (b) the flux ratios or yields, namely, the maximum quantum yield of primary photochemistry ($\varphi_{Po} = TR_0/ABS$), the efficiency ($\psi_0 = ET_0/TR_0$) with which a trapped exciton can move an electron into the electron transport chain further than Q_A^- and the quantum yield of electron transport ($\varphi_{Eo} = ET_0/ABS = \varphi_{Po} \times \psi_0$), (c) the phenomenological energy fluxes (per excited cross-section, CS) for absorption (ABS/CS), trapping (TR_0/CS), dissipation (DI_0/CS) and electron transport (ET_0/CS). The amount of active PSII reaction centres per excited cross-section (RC/CS) is also derived by the JIP-test. [Note: the calculation of the phenomenological fluxes is based on the ABS/CS flux, which can be directly determined (as Chl/area or Chl/dry weight or Chl/protein) or approximated by F_0 or F_M].

Figure 21.7 depicts also the definition of the performance index on an absorption basis, PI_{ABS}, which compiles all basic biophysical parameters and, as well

► **Fig. 21.7** Conversion of fluorescence data selected from an O-J-I-P fluorescence transient to biophysical parameters with the JIP-test, which is based on the Theory of Energy Fluxes in Biomembranes. The figure distinguishes experimental signals, normalised signals and biophysical parameters, the latter being further distinguished in specific and phenomenological fluxes and yields (or flux ratios). The definition of the performance index on absorption basis, PI_{ABS}, is also depicted, together with the formulae which link the PI_{ABS} with the experimental and normalised signals and the biophysical parameters. (Chl_{RC} and Chl_{ant} stand for the chlorophyll content of the reaction centers and of the antenna respectively, while $Chl_{total} = Chl_{ant} + Chl_{RC}$ stands for the total chlorophyll; for the definition of other symbols, see text, Table 21.1 and Fig. 21.5)

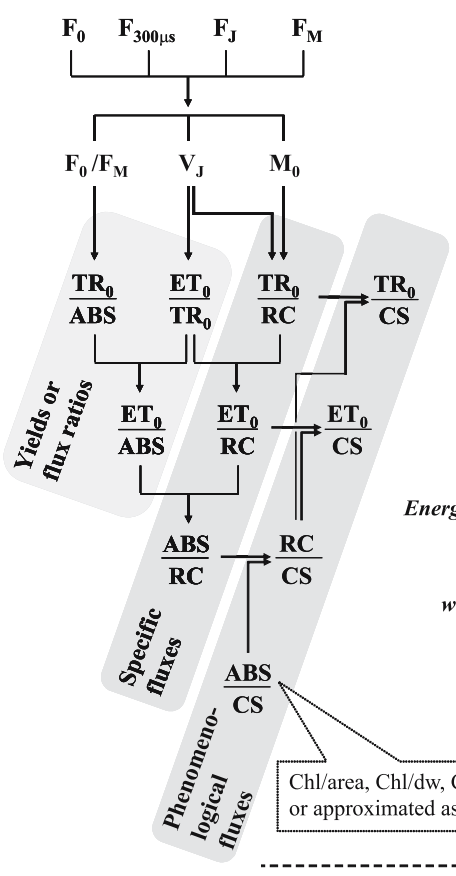

Biophysical expressions derived by the Energy Flux Theory and calculated with the JIP-test

Experimental signals

$$PI_{ABS} = \frac{1-(F_0/F_M)}{4(F_{300\mu s}-F_0)/(F_J-F_0)} \cdot \frac{(F_M-F_0)}{F_0} \cdot \frac{(F_M-F_J)}{(F_J-F_0)}$$

Normalised signals

$$PI_{ABS} = \frac{(F_V/F_M)}{M_0/V_J} \cdot \frac{F_V}{F_0} \cdot \frac{1-V_J}{V_J}$$

$$PI_{ABS} = \frac{RC}{ABS} \cdot \frac{TR_0}{DI_0} \cdot \frac{ET_0}{TR_0-ET_0}$$

DEFINITION OF PERFORMANCE INDEX PI_{ABS}

$$PI_{ABS} = \frac{\gamma_{RC}}{1-\gamma_{RC}} \cdot \frac{\varphi_{Po}}{1-\varphi_{Po}} \cdot \frac{\psi_o}{1-\psi_o}$$

$$\gamma_{RC} \equiv \frac{Chl_{RC}}{Chl_{RC}+Chl_{ant}} = \frac{Chl_{RC}}{Chl_{total}} \Rightarrow \frac{\gamma_{RC}}{1-\gamma_{RC}} = \frac{Chl_{RC}}{Chl_{ant}} \sim \frac{RC}{ABS}$$

$$\varphi_{Po} \equiv \frac{TR_0}{TR_0+DI_0} = \frac{TR_0}{ABS} \Rightarrow \frac{\varphi_{Po}}{1-\varphi_{Po}} = \frac{TR_0}{DI_0}$$

$$\psi_0 \equiv \frac{ET_0}{TR_0} \Rightarrow \frac{\psi_o}{1-\psi_o} = \frac{ET_0}{TR_0-ET_0}$$

documented (for reviews, see Strasser et al. 2000, 2004), is a very appropriate representative index of the vitality of the photosynthetic system – macrostate:

$$PI_{ABS} = \frac{\gamma_{RC}}{1-\gamma_{RC}} \cdot \frac{\varphi_{Po}}{1-\varphi_{Po}} \cdot \frac{\psi_o}{1-\psi_o}$$

where $\gamma_{RC} = Chl_{RC}/Chl_{total}$, hence $\gamma_{RC}/(1-\gamma_{RC}) = Chl_{RC}/Chl_{total} \sim RC/ABS$.

According to the definition, the performance index is a product of expressions of the form $[p_i/(1-p_i)]$, where the several p_i stand for probabilities or fractions. Such expressions are well known in chemistry, with p_i representing e.g. the fraction of the reduced and $(1-p_i)$ the fraction of the oxidised form of a compound, in which case $\log[p_i/(1-p_i)]$ expresses the potential or driving force for the corresponding oxido-reduction reaction (Nernst's equation). Extrapolating this inference from chemistry, we can define the $\log(PI_{ABS})$ as the total driving force (DF_{ABS}) for photosynthesis of the observed system, created by summing up the partial driving forces for each of the several energy bifurcations (all at the onset of the fluorescence rise O-J-I-P).

$$DF_{ABS} = \log(PI_{ABS}) = \log\left(\frac{RC}{ABS}\right) + \log\left(\frac{\varphi_{Po}}{1-\varphi_{Po}}\right) + \log\left(\frac{\psi_o}{1-\psi_o}\right)$$

By presenting a clear distinction between experimental signals, normalised signals and biophysical parameters, Fig. 21.7 depicts also how PI_{ABS} can be directly calculated using any of these sets.

21.3 Case Study

21.3.1 Mycorrhization and the Advantages of *Piriformospora indica*, an Emerging Growth Booster

The beneficial role of arbuscular mycorrhiza fungi (AMF) is well documented. *P. indica*, which belongs to the Basidiomycota, is a newly described root endophyte (Verma et al. 1998) with AMF-like characteristics (Varma et al. 2001). Moreover, in contrast to AMF which are obligate endosymbionts, *P. indica* has the added advantage of being able to grow in axenic cultures – it is cultivable in vitro (Varma et al. 1999).

P. indica has growth- and yield-promoting effects on a broad range of plants, including medicinal plants: shoot and root length, biomass, basal stem, leaf area, overall size, number of inflorescences and flowers and seed production are all enhanced in the presence of fungi (Rai et al. 2001). Inoculation with the fungus and application of fungal culture filtrate also increase tolerance to temperature and drought, as well as to heavy metals. For example, concerning cadmium, which exerts toxic effects on plants, *P. indica* provides alleviation of the causative stress (tolerance up to 300 μg Cd per gramme of air-dried soil). Moreover, *P. indica* has the properties of biofertilizer, bioregulator, phytoremediator, immunomodulator and antioxidants/drugs enhancer (Varma, personal communication). It also provides biocontrol against insects and pathogens (Pham et al. 2004a, b, c).

All these impressive traits make *P. indica* very valuable, both for basic research, as an excellent model organism for the study and understanding of the beneficial plant-microbe interactions and for applied research, as a powerful new candidate tool for improving plant production systems in agroforestry and flori-horticulture applications for sustainable agriculture.

We here apply our approach for a comparative study of the beneficial role of typical arbuscular mycorrhiza fungi (*G. mosseae*, *G. caledonium*) and *P. indica*, on chick peas (*Cicer arietinum* L. Chafa variety) exposed to cadmium stress.

21.3.2 Phenomics of the O-J-I-P Fluorescence Transient for the Study of Cadmium Stress on Chick Peas (*Cicer arietinum* L. Chafa variety) With and Without Symbiosis With *Glomus mosseae*, *G. caledonium* and *Piriformospora indica*

As analysed above (Fig. 21.6), normalisations and differences of the fluorescence transients reveal a deconvolution of the typical O-J-I-P shape into additional bands, carrying useful information about microstates of the photosynthetic system.

Figure 21.8 is an application of this approach to the presented case study. O-J-I-P Chl *a* fluorescence transients are plotted as kinetics of the relative variable fluorescence $W_t = V_t/V_J = (F_t–F_0)/(F_J–F_0)$ on a logarithmic time-scale (like in the lower panel of Fig. 21.4). The presented transients were exhibited by dark-adapted leaves of chickpea (*C. arietinum* L. Chafa variety) measured with the Handy-PEA fluorimeter at the 42nd day after inoculation with *G. mosseae* (black diamonds), *G. caledonium* (black squares) and *P. indica* (black circles). All inoculated plants were under cadmium stress (added on the 21st day). The transients from non-inoculated plants of the same age in the absence (control, grey circles) or presence of Cd (black triangles) are also depicted. We observe that these transients *(open symbols)* show minor differences (similarly to the

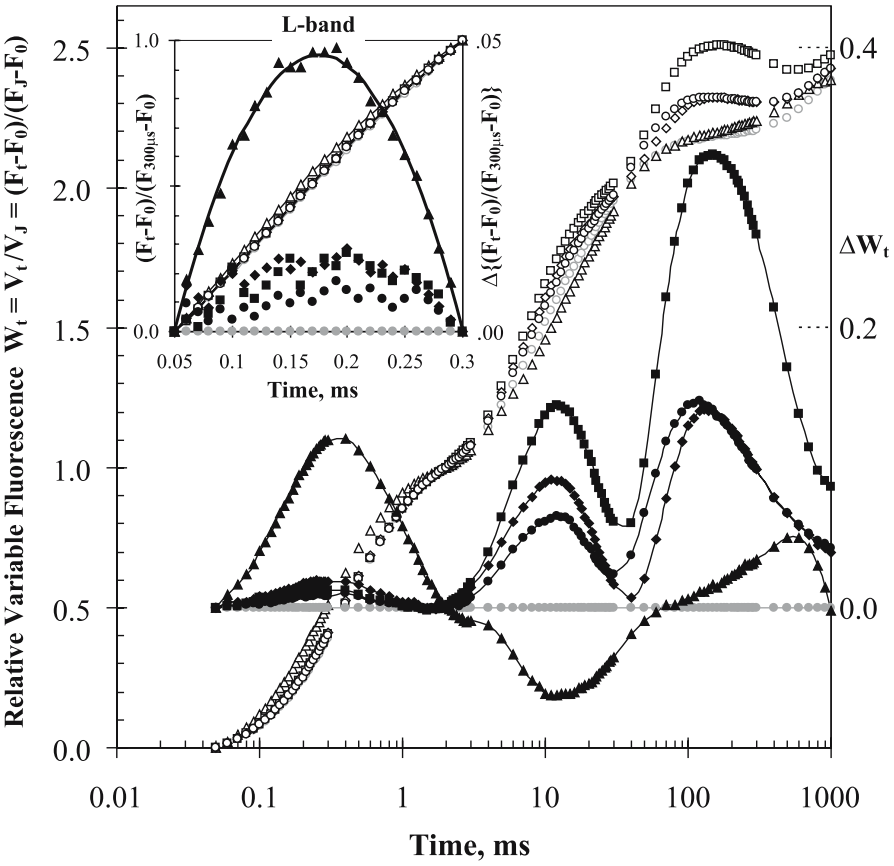

Fig. 21.8 Chl *a* fluorescence transients (each presenting average kinetics of raw fluorescence data from 12 samples) of dark-adapted leaves of chick peas (*Cicer arietinum* L. Chafa variety) measured with the Handy-PEA fluorimeter at the 42nd day after inoculation with *G. mosseae* (*black diamonds*), *G. caledonium* (*black squares*) and *P. indica* (*black circles*). All inoculated plants were under cadmium stress (added on the 21st day). The transients from non-inoculated plants of the same age in the absence of Cd (control, *grey circles*) or presence of Cd (*black triangles*) are also depicted. The transients are presented as kinetics of the relative variable fluorescence $W_t = V_t/V_J = (F_t–F_0)/(F_J–F_0)$, *open symbols*, *left axis*, and as ΔW_t (treated minus control; *closed symbols*, *right axis*). The insert depicts, on a linear time-scale from 50 μs to 300 μs, the transients normalised as $(F_t–F_0)/(F_{300\mu s}–F_0)$, as well as their differences $\Delta[(F_t–F_0)/(F_{300\mu s}–F_0)]$ from the control, which reveal the L-band

cases presented in Figs. 21.4, 21.6). However, when plotted as difference kinetics ΔW_t (treated minus control; closed symbols), they reveal major differences concerning the amplitudes of the bands. The difference kinetics demonstrate that: (a) the trend of the impact of all three symbionts is the same and (b) this impact is the almost complete elimination (range 50 μs to 2 ms) or even the overcompensation (2 ms to 1 s) of the major effects of Cd stress on the transients. Similar information is derived from the insert of Fig. 21.8, where the transients are de-

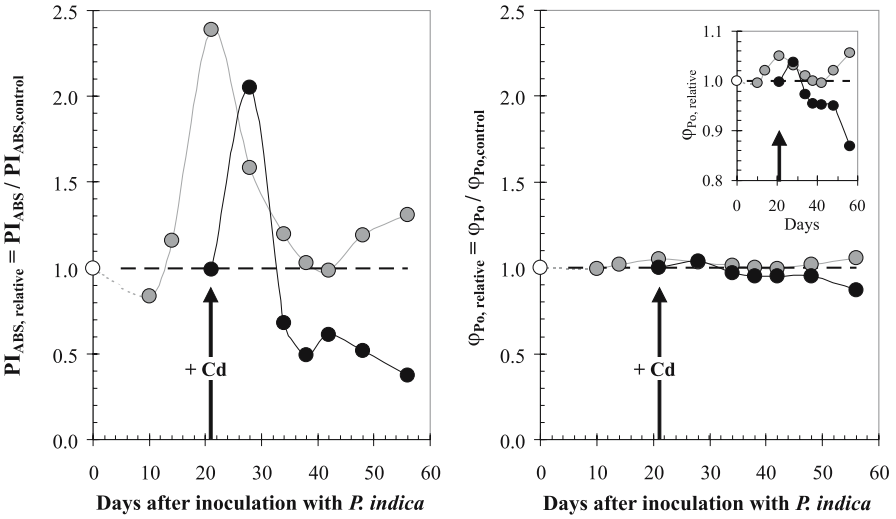

Fig. 21.9 The relative performance index $PI_{ABS}/PI_{ABS,control}$ (*left panel*) and the relative maximum quantum yield of primary photochemistry $\varphi_{Po}/\varphi_{Po,control}$ (*right panel*), from day 10 to day 56 after inoculation of chick peas (*C. arietinum* L. Chafa variety) plants with *P. indica*. Inoculated (*grey circles*) and non-inoculated (*black circles*) plants were put under cadmium stress on the 21st day. The value of the parameter from non-inoculated, and without addition of cadmium, plants of the same age was used as the control value of each parameter (subscript "*control*")

picted, on a linear time-scale from 50 μs to 300 μs, as $(F_t–F_0)/(F_{300\mu s}–F_0)$, along with their difference $\Delta[(F_t–F_0)/(F_{300\mu s}–F_0)]$ from the control. It is worth noting that, when this normalisation is used, the difference transients reveal the L-band (not appearing in ΔW_t; see legend of Fig. 21.6).

Let us now follow the impact of Cd stress with and without symbiosis on parameters derived by the JIP-test.

We first demonstrate a comparison of the impact of *P. indica* on the performance index PI_{ABS} (for definition and formulae, see Fig. 21.7) and the commonly used maximum quantum yield of primary photochemistry φ_{Po} (for definition and formulae see Table 21.1) by depicting in Fig. 21.9 their stress kinetics from day 10 to day 56 after inoculation with *P. indica*. Inoculated (grey circles) and non-inoculated plants (black circles) were put under cadmium stress on the 21st day. The parameters are presented as $PI_{ABS}/PI_{ABS,control}$ (left panel) and $\varphi_{Po}/\varphi_{Po,control}$ (right panel), where $PI_{ABS,control}$ and $\varphi_{Po,control}$ refer to non-inoculated plants of the same age that were not put under cadmium stress (control plants).

We observe that the $PI_{ABS}/PI_{ABS,control}$ undergoes wide changes during the course of the stress. Though Cd addition is shown to affect both non-inoculated and inoculated plants, the beneficial role of the symbiont concerning the tolerance to Cd stress is clearly revealed. $\varphi_{Po}/\varphi_{Po,control}$ appears much less sensitive than $PI_{ABS}/PI_{ABS,control}$ and thus much less appropriate in detecting vitality

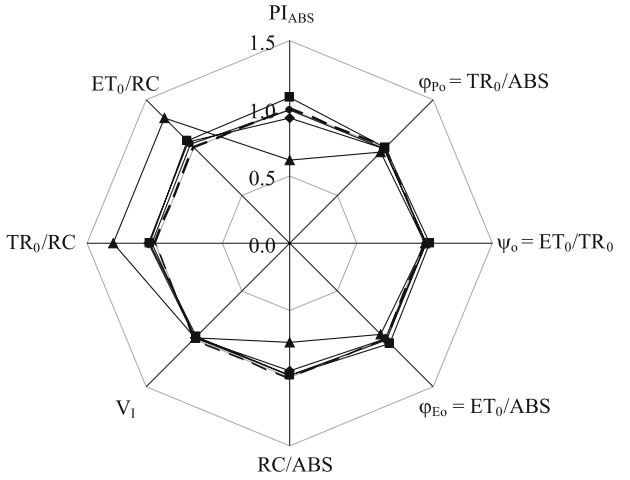

Fig. 21.10 The impact of cadmium stress on different parameters derived by the JIP-test from the fluorescence transients (for terms, definitions and formulae, see Section 21.2.4.4, also Fig. 21.5 and Table 21.1). The figure refers to the 42nd day after inoculation with *G. mosseae* (*diamonds*), *G. caledonium* (*squares*) and *P. indica* (*circles*). All inoculated plants were under cadmium stress (added on the 21st day). The case of non-inoculated plants of the same age under cadmium stress is also depicted (*triangles*). Each case is represented by an octagon, where the value of each parameter is normalised on that of the control case (i.e. non-inoculated, and without addition of cadmium, plants of the same age), which is thus depicted by the regular octagon (*dashed thick line*)

changes. However, magnification of the changes it undergoes (as shown in the insert) reveals that it exhibits a trend similar to that of $PI_{ABS}/PI_{ABS,control}$ for both non-inoculated and inoculated plants.

The spider-plot of Fig. 21.10 presents the impact of cadmium stress on different parameters derived by the JIP-test from the fluorescence transients, for non-inoculated and inoculated (with the three symbionts) plants. The parameters are: PI_{ABS}, φ_{Po}, ψ_o, φ_{Eo}, RC/ABS, V_I, TR_0/RC and ET_0/RC (see text in Section 21.2.4.4, also Fig. 21.5 and Table 21.1). The figure refers to the 42nd day after inoculation with *G. mosseae* (diamonds), *G. caledonium* (squares) and *P. indica* (circles). All inoculated plants were under cadmium stress (added on the 21st day). Non-inoculated plants of the same age under cadmium stress are also depicted (triangles). Each case is represented by an octagon, where the value of each parameter is normalised on that of the control case (i.e. non-inoculated, and without addition of cadmium, plants of the same age), which is thus depicted by the regular octagon (dashed thick line).

Further than depicting in a comparative way the quantitative impact of stress on the individual parameters, each of which is linked to microstates, the presentation of the results with a spider-plot has the advantage of providing an easy

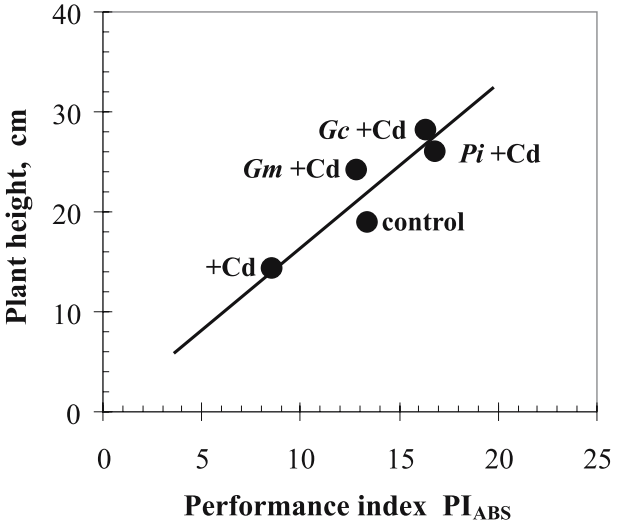

Fig. 21.11 Correlation of the height of the plant (physiological parameter) and the performance index PI_{ABS} (biophysical parameter) derived by the JIP-test, for non-inoculated chick peas (*C. arietinum* L. Chafa variety) plants in the absence (*control*) or presence (+*Cd*) of cadmium, or inoculated with *G. mosseae*, *G. caledonium* and *P. indica* and exposed to cadmium stress (*Gm*+Cd, *Gc*+Cd and *Pi*+Cd, respectively)

recognition of stress effects. We can immediately see the distortion from the regular octagon (control) caused by Cd (triangles), which can be registered as the characteristic pattern of Cd stress; and we can also see that, for plants in symbiosis with any of the three symbionts, almost no distortion from the control pattern (regular octagon) occurs.

21.3.3 Correlation of Physiological with Biophysical Parameters

Further than proving the high sensitivity of the performance index, we also checked whether and how it is related with physiological parameters, commonly used for the evaluation of the impact of symbiosis on the vitality of plants. Figure 21.11 shows indeed a striking correlation between the height of the plant and the performance index PI_{ABS}. The data presented come from non-inoculated chick peas (*C. arietinum* L. Chafa variety) plants in the absence *(control)* and presence (+Cd) of cadmium, as well as from plants inoculated with *G. mosseae*, *G. caledonium* and *P. indica* and exposed to cadmium stress (*Gm*+ Cd, *Gc*+ Cd and *Pi*+ Cd, respectively).

21.4 Conclusions

Biophysical phenomics, as we term our approach, here applied for the evaluation of the effectiveness of mycorrhization, is shown to be powerful for the description of an in vivo vitality analysis (behaviour/performance) of PSII, i.e. for the description of a biophysical phenotype (macrostate), as well as for the recognition and evaluation of stress impacts on microstates (the functional building blocks into which the macrostate is deconvoluted). With this approach we demonstrate the beneficial role of typical AMF and of the equally effective *P. indica*, concerning tolerance to Cd stress.

Our techniques are thus shown to be very suitable for studying the effectiveness of soil microbial activity. The advantages of these techniques can be summarised as follows:

- They provide an early diagnosis of vitality changes (primary stress effects, hence stress tolerance).
- They can be used to screen not only leaves but any green part of the plant.
- They are rapid – only a few seconds are needed for each measurement.
- They can be applied in vivo.
- They can be carried out anywhere – in the field, in the greenhouse or even in tissue cultures – and even on samples as small as 2 mm^2.
- They are not invasive.
- They are inexpensive.

References

Briantais JM, Vernotte C, Krause GH, Weiss E (1986) Chlorophyll *a* fluorescence of higher plants: chloroplasts and leaves. In: Govindjee, Amesz J, Fork DC (eds) Light emission by plants and bacteria. Academic, New York pp 539–583

Clark AJ, Landolt W, Bucher J, Strasser RJ (1998) The response of *Fagus sylvatica* to elevated CO2 and ozone probed by the JIP-test based on the chlorophyll fluorescence rise OJIP. In: De Kok LJ, Stulen I (eds) Responses of plant metabolism to air pollution and global change. Backhuys, Leiden, pp 283–286

Clark AJ, Landolt W, Bucher J, Strasser RJ (2000) Beech (*Fagus sylvatica*) response to ozone exposure assessed with a chlorophyll *a* fluorescence performance index. Environ Pollut 109:501–507

Dau H (1994) Molecular mechanisms and quantitative models of variable photosystem II fluorescence. Photochem Photobiol 60:1–23

Epitalawage N, Eggenberg P, Strasser RJ (2003) Use of fast chlorophyll a fluorescence technique in detecting drought and salinity tolerant chickpea (*Cicer arietinum* L.) varieties. Arch Sci Genève 56:79–93

Govindjee (1995) Sixty-three years since Kautsky: chlorophyll *a* fluorescence. Aust J Plant Physiol 22:131–160

Govindjee, Amesz J, Fork DC (1986) Light emission by plants and bacteria. Academic, New York

Kautsky H, Hirsch A (1931) Neue Versuche zur Kohlensäureassimilation. Naturwissenschaften 19:964

Krause GH, Weiss E (1991) Chlorophyll fluorescence and photosynthesis: the basics. Annu Rev Plant Physiol Plant Mol Biol 42:313–349

Krüger GHJ, Tsimilli-Michael M, Strasser RJ (1997) Light stress provokes plastic and elastic modifications in structure and function of photosystem II in camellia leaves. Physiol Plant 101:265–277

Ouzounidou G, Moustakas M, Strasser RJ (1997) Sites of action of copper in the photosynthetic apparatus of maize leaves: kinetic analysis of chlorophyll fluorescence, oxygen evolution, absorption changes and thermal dissipation as monitored by photoacoustic signals. Aust J Plant Physiol 24:81–90

Papageorgiou G (1975) Chlorophyll fluorescence: an intrinsic probe of photosynthesis. In: Govindjee (ed) Bioenergetics of photosynthesis. Academic, New York, pp 319–371

Pham GH, Singh A, Malla R, Kumari R, Prasad R, Sachdev M, Luis P, Kaldorf M, Tatjana P, Harrmann S, Hehl S, Declerck S, Buscot F, Oelmuller R, Rexer KH, Kost G, Varma A (2004a) Interaction of *P. indica* with other microorganisms and plants. In: Varma A, Abbott L, Werner D, Hampp R (eds) Plant surface microbiology. Springer, Berlin Heidelberg New York, pp 237–265

Pham GH, Kumari R, Singh A, Sachdev M, Prasad R, Kaldorf M, Buscot F, Oelmuller R, Tatjana P, Weiβ M, Hampp R, Varma A (2004b) Axenic cultures of *Piriformospora indica*. In: Varma A, Abbott L, Werner D, Hampp R (eds) Plant surface microbiology. Springer, Berlin Heidelberg New York, pp 593–616

Pham GH, Srivastava A, Saxena AK, Pareek A, Varma A (2004c) Protocol to understand the interaction between rhizobacteria and symbiotic fungus: *Piriformospora indica*. In: Podila G, Varma A (eds) Basic research and applications: Mycorrhizae. (Microbiology series, vol 1) IK International, New York, pp 425–450

Prakash JSS, Srivastava A, Strasser RJ, Mohanty P (2003) Senescence-induced alterations in the photosystem II functions of *Cucumis sativus* cotyledons: probing of senescence driven alterations of photosystem II by chlorophyll *a* fluorescence induction O-J-I-P transients. Indian J Biochem Biophys 40:160–168

Rai M, Acharya D, Singh A, Varma A. (2001) Positive growth responses of the medicinal plants, *Spilanthus calva* and *Withania somnifera* to inoculation by *Piriformospora indica* in field trials. Mycorrhiza 11:123–128

Schmitz P, Maldonado-Rodriguez R, Strasser RJ (2001) Evaluation of the nodulated status of *Vigna unguiculata* probed by the JIP-test based on the chlorophyll *a* fluorescence rise. In: CSIRO (ed) Proceedings of the 12th international congress on photosynthesis. CSIRO, Collingwood, S36-012

Srivastava A, Strasser RJ (1995) How do land plants respond to stress temperature and stress light? Arch Sci Genève 48:135–145

Srivastava A, Strasser RJ (1996) Stress and stress management of land plants during a regular day. J Plant Physiol 148:445–455

Srivastava A, Guisse B, Greppin H, Strasser RJ (1997) Regulation of antenna structure and electron transport in PS II of *Pisum sativum* under elevated temperature probed by the fast polyphasic chlorophyll *a* fluorescence transient OKJIP. Biochim Biophys Acta 1320:95–106

Strasser RJ (1978) The grouping model of plant photosynthesis. In: Akoyunoglou G (ed) Chloroplast development. Elsevier, Dordrecht, pp 513–524

Strasser RJ (1981) The grouping model of plant photosynthesis: heterogeneity of photosynthetic units in thylakoids. In: Akoyunoglou G (ed) Photosynthesis III. Structure and molecular organisation of the photosynthetic apparatus. Balaban International Science Services, Philadelphia, pp 727–737

Strasser RJ (1985) Dissipative Strukturen als Thermodynamischer Regelkreis des Photosyntheseapparates. Ber Deutsche Bot Ges Bd 98:53–72

Strasser RJ, Govindjee (1992) The F0 and the O-J-I-P fluorescence rise in higher plants and algae. In: Argyroudi-Akoyunoglou JH (ed) Regulation of chloroplast biogenesis. Plenum, New York pp 423–426

Strasser RJ, Tsimilli-Michael M (1998) Activity and heterogeneity of PS II probed in vivo by the chlorophyll *a* fluorescence rise O-(K)-J-I-P. In: Garab G (ed) Photosynthesis: mechanisms and effects, vol V. Kluwer Academic, Rotterdam, pp 4321–4324

Strasser RJ, Tsimilli-Michael M (2001) Stress in plants, from daily rhythm to global changes, detected and quantified by the JIP-test. Chim Nouv 75:3321–3326

Strasser RJ, Tsimilli-Michael M (2005) State-changes realising adaptation to stress as the result of an optimized redistribution of functional microstates. In: van Est A, Bruce D (eds) Photosynthesis: fundamental aspects to global perspectives. Allen, Montreal, pp 537–540

Strasser RJ, Srivastava A, Govindjee (1995) Polyphasic chlorophyll *a* fluorescence transient in plants and cyanobacteria. Photochem Photobiol 61:32–42

Strasser RJ, Srivastava A, Tsimilli-Michael M (2000) The fluorescence transient as a tool to characterize and screen photosynthetic samples. In: Yunus M, Pathre U, Mohanty P (eds) Probing photosynthesis: mechanism, regulation and adaptation. Taylor and Francis, London, pp 443–480

Strasser RJ, Tsimilli-Michael M, Srivastava A (2004) Analysis of the chlorophyll *a* fluorescence transient. In: Papageorgiou GC, Govindjee (eds) Chlorophyll fluorescence: a signature of photosynthesis. (Advances in photosynthesis and respiration series, vol 19) Kluwer Academic, Rotterdam, pp 321–362

Tóth SZ, Schansker G, Strasser RJ (2005) In intact leaves, the maximum fluorescence level (FM) is independent of the redox state of the plastoquinone pool: a DCMU-inhibition study. Biochim Biophys Acta 1708:275–282

Tsimilli-Michael M, Strasser RJ (2001) Fingerprints for climate changes on the behaviour of the photosynthetic apparatus, monitored by the JIP-test. A case study on light and heat stress adaptation of the symbionts of temperate and coral reef foraminifers in hospite. In: Walther G-R, Burga CA, Edwards PJ (eds) Fingerprints of climate changes – adapted behaviour and shifting species ranges. Kluwer, New York, pp 229–247

Tsimilli-Michael M, Strasser RJ (2002) Mycorrhization as a stress adaptation procedure. In: Gianinazzi S, Haselwandter K, Schüepp H, Barea JM (eds) Mycorrhiza technology in agriculture: from genes to bioproducts. Birkhauser, Basel, pp 199–209

Tsimilli-Michael M, Krüger GHJ, Strasser RJ (1995) Suboptimality as driving force for adaptation: a study about the correlation of excitation light intensity and the dynamics of fluorescence emission in plants. In: Mathis P (ed) Photosynthesis: from light to biosphere, vol V. Kluwer Academic, Rotterdam, pp 981–984

Tsimilli-Michael M, Krüger GHJ, Strasser RJ (1996) About the perpetual state changes in plants approaching harmony with their environment. Arch Sci Genève 49:173–203

Tsimilli-Michael M, Pêcheux M, Strasser RJ (1998) Vitality and stress adaptation of the symbionts of coral reef and temperate foraminifers probed in hospite by the fluorescence kinetics O-J-I-P. Arch Sci Genève 51:1–36

Tsimilli-Michael M, Pêcheux M, Strasser RJ (1999) Light and heat stress adaptation of the symbionts of temperate and coral reef foraminifers probed in hospite by the chlorophyll a fluorescence kinetics O-J-I-P. Z Naturforsch 54C:671–680

Tsimilli-Michael M, Eggenberg P, Biro B, Köves-Pechy K, Vörös I, Strasser RJ (2000) Synergistic and antagonistic effects of arbuscular mycorrhizal fungi and *Azospirillum* and *Rhizobium* nitrogen-fixers on the photosynthetic activity of alfalfa, probed by the chlorophyll *a* polyphasic fluorescence transient O-J-I-P. Appl Soil Ecol 15:169–182

Van Rensburg L, Krüger GHJ, Eggenberg P, Strasser RJ (1996) Can screening criteria for drought resistance in *Nicotiana tabacum* L. be derived from the polyphasic rise of the chlorophyll *a* fluorescence transient (OJIP)? S Afr J Bot 62:337–341

Van Heerden PDR, Tsimilli-Michael M, Krüger GHJ, Strasser RJ (2003) Dark chilling effects on soybean genotypes during vegetative development: parallel studies of CO2 assimilation, chlorophyll *a* fluorescence kinetics O-J-I-P and nitrogen fixation. Physiol Plant 117:476–491

Varma A, Verma S, Sudha, Sahay N, Britta B, Franken P (1999) *Piriformospora indica* – a cultivable plant growth promoting root endophyte with similarities to arbuscular mycorrhizal fungi. Appl Environ Microbiol 65:2741–2744

Varma A, Singh A, Sudha, Sahay N, Sharma J, Roy A, Kumari M, Rana D, Thakran S, Deka D, Bharti K, Franken P, Hurek T, Blechert O, Rexer K-H, Kost G, Hahn A, Hock B, Maier W, Walter M, Strack D, Kranner I (2001) *Piriformospora indica*: a cultivable mycorrhiza-like endosymbiotic fungus. In: Varma A, Hock B (eds) Mycota IX. Springer, Berlin Heidelberg New York, pp 123–150

Verma S, Varma A, Rexer K-H, Hassel A, Kost G, Sarbhoy A, Bisen P, Buetehorn P, Franken P (1998) *Piriformospora indica* gen. nov., a new root-colonizing fungus. Mycologia 90:895–909